Tissue Engineering

DOI: 10.1002/anie.201102249

# High-Density, Multiplexed Patterning of Cells at Single-Cell Resolution for Tissue Engineering and Other Applications**

*Udi Vermesh, Ophir Vermesh, Jun Wang, Gabriel A. Kwong, Chao Ma, Kiwook Hwang, and James R. Heath**

The ability to arrange distinct cells in specific, predefined patterns at single-cell resolution could have broad applications in tissue engineering, cell-based assays, cell and tissue co-cultures, and fundamental studies of cell–cell interactions. In particular, the proper functioning of engineered constructs for tissue and organ transplantation requires positioning different cell types in anatomically precise arrangements that mimic their microarchitectural configurations in native tissues. Existing methods for micrometer-scale cell patterning include microcontact printing,[1] inkjet printing,[2,3] elastomeric stencils,[4] dielectrophoresis,[5,6] and others.[7,8] The major limitation of most existing platforms, however, is that either they cannot be straightforwardly scaled for highly multiplexed cell patterning, or they do not offer single-cell patterning precision and control, or both.

We report on the microfluidic-guided flow-patterning of surfaces as an avenue for constructing tissues. While microfluidic channels have been previously utilized to spatially control the deposition of biomolecules onto a surface as one-dimensional stripes,[9] patterns of arbitrary, two-dimensional complexity at single cell resolution are more challenging. We report on three advances to achieve such patterns. First, we execute two sequential steps of microfluidic flow patterning, one at right angles with the other, such that the intersections of the flow patterned DNA stripes constitute an $n \times m$ array of unique elements, where $n$ and $m$ are the respective numbers of microchannels utilized for each of the two flow patterning steps. Second, the set of ssDNA oligomers used in the second flow-patterning step is designed so that each of the resulting $n \times m$ array elements has a unique molecular identity. Third, we introduce a cell-surface marker-independent chemistry for labeling cells to enable specific cells to be captured at specific spots within the $n \times m$ array (Figure 2). These advances, when integrated together, enable the construction of tissues with architectural precision at the single cell level.

Dense microarrays with cell-sized DNA features were created as shown in Figure 1a. A PDMS mold containing 20 parallel 10 μm-wide channels at 30 μm pitch was used to flow-pattern three distinct 80-mer ssDNA "anchor" strands (**A, B**, and **C**) in adjacent sets of three channels (one distinct strand per channel) onto a polylysine-coated glass surface. The PDMS mold was then rotated 90°, and sets of nine distinct ssDNA "bridge" oligomers (**A′-i**, **B′-ii**, …) were flow-patterned at right angles across the first pattern (three distinct strands per channel). Each bridge oligomer includes a 20-base pair tail that is complementary to one of the three anchor sequences, and a 20-base pair head with a unique sequence. As such, once the flow-patterning was complete, the resultant $3 \times 3$ arrays (Figure 1b) contained nine distinct oligonucleotide head sequences (**i**–**ix**) that were available to bind distinct cell types conjugated to one of nine complementary strands (**i′**–**ix′**). By adding only **A′-i**, **B′-ii**, and **C′-iii** strands in the

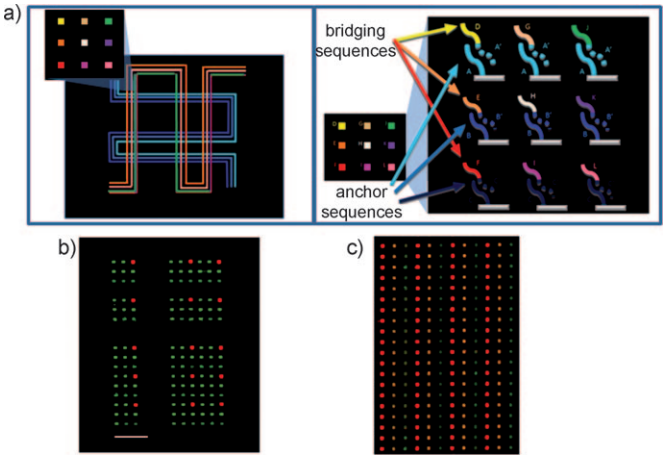


***Figure 1.*** Preparation of a high-density DNA microarray for tissue assembly. a) Orientation of microfluidic flow patterning mold #1 (blue lines) for deposition of $n$ anchor ssDNA sequences, and #2 (red lines) for pattering $m$ bridging sequences. The resulting pattern is a series of $n \times m$ microarrays, with each array spot having its own unique chemical identity. b) Fluorescent scan of high-density $3 \times 3$ DNA microarrays is shown. Red spots = **i** oligomer (hybridized with **i′**-Cy5); green spots = **ii**, **iii**, **iv**, **v**, **vi**, **vii**, **viii**, and **ix** oligomers (hybridized with **ii′**–**ix′**-Cy3). Scale bar: 100 μm. c) Fluorescent scan of $3 \times 1$ arrays. Red = oligonucleotide **i**; yellow = oligonucleotide **ii**; green = oligonucleotide **iii**. Red, green, and yellow spots were created by adding **i′**-Cy5, **iii′**-Cy3, and equal concentrations of **ii′**-Cy5 and **ii′**-Cy3, respectively.

[*] U. Vermesh,[+] O. Vermesh,[+] J. Wang, G. A. Kwong,[$] C. Ma, K. Hwang, Prof. J. R. Heath
Division of Chemistry and Chemical Engineering
California Institute of Technology
1200 E. California Boulevard, Pasadena, California, 91125 (USA)
E-mail: heath@caltech.edu
Homepage: http://www.its.caltech.edu/~heathgrp

[$] Current Address: Harvard-Massachusetts Institute of Technology Division of Health Sciences & Technology, Cambridge, MA 02139 (USA)

[+] These authors contributed equally to this work.

[**] This work was funded by the National Cancer Institute Grant No. 5U54 CA119347 (JRH PI) and by generous support from the Ivy Foundation and the Grand Duchy of Luxembourg, via a subcontract from the Institute for Systems Biology. We thank Integrated Sensing Systems, Inc. for help with silicon hard mold fabrication and M. Di Franco for technical assistance.

Supporting information for this article is available on the WWW under http://dx.doi.org/10.1002/anie.201102249.

second patterning step, 3×1 arrays could also be created (Figure 1c). The feature size, pitch, and shape of these DNA array features can be controlled by adjusting the microfluidic channel widths, inter-channel distances, and channel geometries, respectively. We used 10 μm wide PDMS flow-patterning channels at 30 μm pitch, resulting in closely packed 10 μm × 10 μm DNA squares that could each accommodate a single cell. However, DNA feature sizes can easily be adjusted to accommodate larger cells or cell clusters.

In order to convert our DNA arrays into cell arrays, we explored a new cell surface marker-independent method for labeling each cell type with a unique complementary oligonucleotide strand (**i′**, **ii′**, …), building on previous cell encoding strategies.[10,11] In our approach, cell membrane proteins were biotinylated and then addressed via cysteine-engineered streptavidin (SaC)-conjugated oligonucleotides (Figure 2).[12,13] To tailor this strategy for DNA conjugation of cells, cell membrane proteins were first biotinylated (by reacting with NHS-biotin), followed by incubation with their respective SaC-DNA oligomers. The advantage of this method is its modularity and ease. The reaction between the SaC constructs and the biotinylated cells occurs immediately upon mixing, so any biotinylated cell can be instantly conjugated with a selected oligomer.

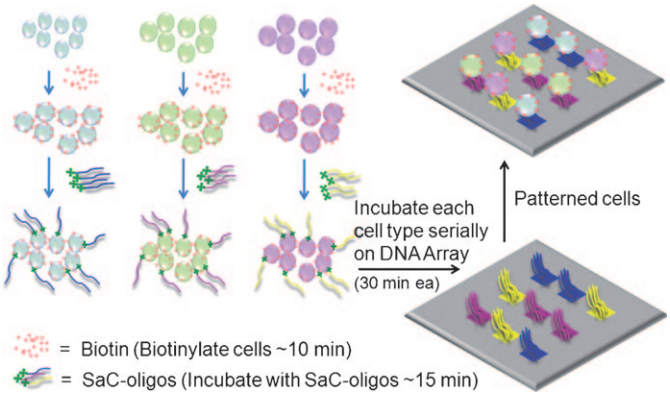


***Figure 2.*** Cell-encoding and assembly. Defined cell types are biotinylated and then addressed with distinct streptavidin (SaC)-conjugated oligonucleotide sequences. The cells are then serially dispensed onto an oligonucleotide-patterned slide, where each individual cell locates to a single cognate spot.

We created a human central nervous system co-culture model by co-assembling neurons and astrocytes into designed structures. We first separately demonstrated the spatially selective capture of single astrocytes and single neurons. Primary human astrocytes were encoded with **ii′** DNA and then incubated onto a 3×3 DNA microarray. The astrocytes localized only to the **ii** DNA spots (Figure 3a), with approximately 27% of those spots bound by one astrocyte each. The fraction of spots bound by two astrocytes was larger (ca. 40%) because the astrocytes exhibited rapid division in culture and they continued to divide following patterning (Figure 3a and Supporting Information, Figure S1). Nonspecific binding of cells to non-cognate spots or to other portions of the slide was not observed. In a separate experiment, primary human

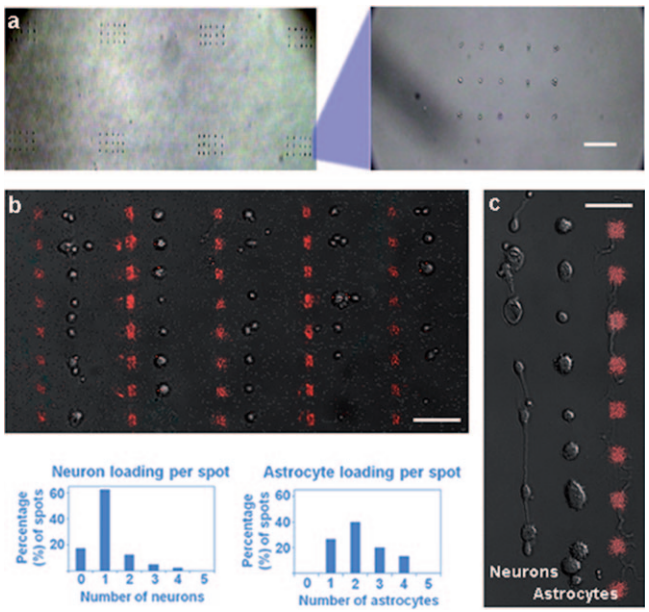


***Figure 3.*** Construction of human neuron-astrocyte assemblies. a) Primary human astrocytes were patterned onto oligonucleotide **ii** spots in a 3×3 array. Consistent patterning is seen in the left (low-resolution) image of 8 3x3 arrays; the right image shows a single array. Scale bar: 100 μm. b) Primary human neurons were patterned onto oligonucleotide **iii** spots on a 3×1 array. The fluorescent alignment marker spots were generated by selective hybridization of fluorophore-labeled oligonucleotides to oligonucleotide **i** spots. Scale bar: 50 μm. c) Human astrocytes (middle column) are patterned alongside human neurons from (b) (left column). Scale bar: 30 μm. Histograms depict the distribution of cell loading per spot.

neurons were patterned onto the **iii** DNA spot of a 3×1 microrarray (consisting only of oligonucleotide sequences **i**, **ii**, and **iii** as the capture sequences) to illustrate how densely cells can be patterned (Figure 3b). A much higher percentage of the DNA spots (60%) were bound by only one cell since the neurons do not divide in culture. When reassessed after a 2 day incubation in 37°C media, neuronal processes were observed to be actively growing, demonstrating cell viability. Primary human astrocytes conjugated to **ii′** DNA were then incubated with the neuron-patterned slide and localized to their cognate spots. Viability assays for those cells are presented in the Supporting Information, Figure S1. Based on cell morphology, it was clear that the astrocytes localized to the **ii** DNA spots, while neurons remained on their original **iii** DNA spots, with multiple rows of neurons and astrocytes spaced 30 μm apart (Figure 3c).

We also explored the construction of model pancreatic tissues as an avenue toward engineering islets for type 1 diabetics. We created an islet construct that included mouse α and β islet cell lines patterned on the **iii** and **ii** DNA spots, respectively, of a 3×1 microarray (Figure 4). The α and β cells localized to their cognate DNA spots, typically averaging around 1 cell per spot (ca. 67% of **iii** spots bound one α-cell; ca. 87% of **ii** spots bound one β cell) (Figure 4a,b). For every 100 correctly patterned cells, only one cell bound nonspecifically.

We designated a fraction of our arrays for conducting functional assays by hybridizing DNA conjugated anti-insulin antibodies on spots adjacent to the patterned islet cells.

  

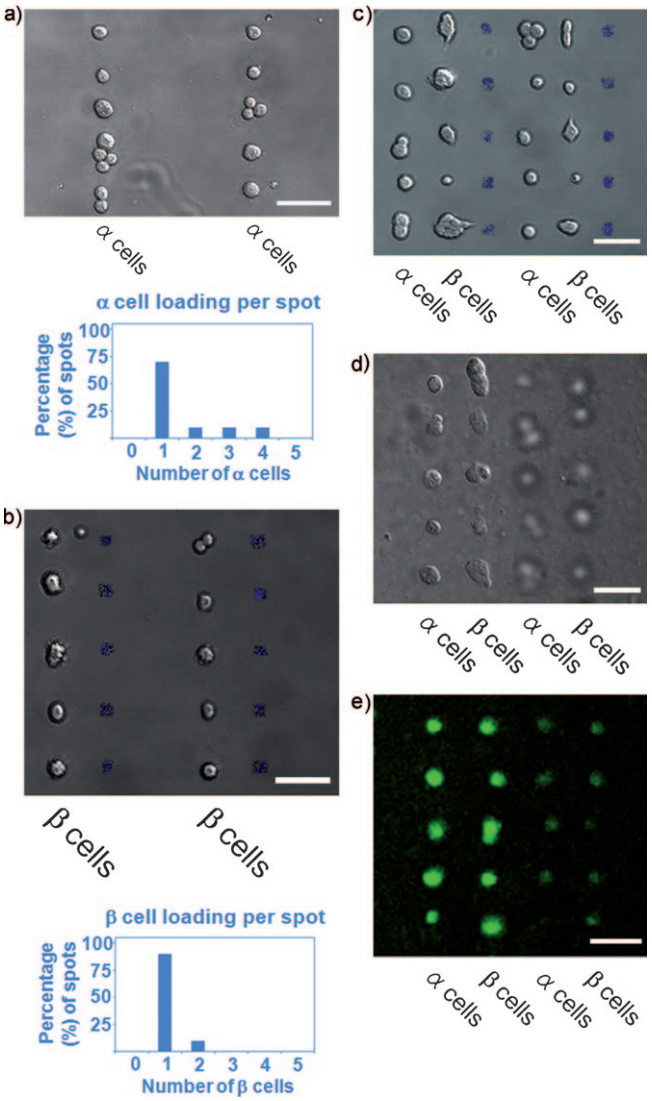


***Figure 4.*** Patterning of mouse α and β islet cells in 2 and 3 dimensions, integrated with assays for insulin production. a) Mouse α cells are patterned on one array column, while a second column (oligonucleotide **i**) was encoded with an immunoassay for insulin production. No insulin is observed from the α cells. b) Similarly patterned mouse β cells yield finite insulin signal (blue spots). c) Integrated mouse α and β cells and insulin assays. d) Patterned α and β cells encased within a 3D stack, with the buried layer of cells slightly out of focus. e) Viability assay of islet cells within the hydrogel construct shown in (d) after one week in 37 °C media. Green fluorescence is attributed to uptake of calcein AM in live cells. The buried layer of cells is slightly out of focus. Scale bars: 30 μm.

Insulin assays were done 2 days after cell assembly. The insulin assays were developed with biotinylated secondary antibodies followed by fluorophore-conjugated streptavidin. The antibody squares fluoresced under confocal microscopy only when β cells (insulin-producers) were present (Figure 4a–c). This technique is amenable to multiplexed secreted-protein assays from single cells due to the multiple unique spots neighboring each cell.

Finally, we built 3D islet tissue constructs from our patterned cells. Unlike in previous studies of cells encased and stacked in UV-curable PEG hydrogel layers,[5,14] our patterned cells were chemically attached to the slide surface via DNA hybridization, so it was not obvious that the cells could be readily transferred into a gel. We found that after encasing cells in such a hydrogel, the cell-laden gel layer could be removed from the glass surface without disturbing the cell pattern or damaging the cells. We aligned and stacked two such hydrogel layers to create a model 3D islet tissue construct (Figure 4d), though multi-layer structures can be created in similar fashion. Viability of the encased cells, as determined by calcein AM/ethidium homodimer (live/dead) staining, was confirmed after incubation in 37 °C media for one week (Figure 4e).

In summary, dense DNA microarrays were used for multiplexed patterning of cells at single-cell resolution using a novel DNA-encoding methodology. Two cell patterns, one made up of two human CNS cell types (neurons and astrocytes) and one consisting of two mouse pancreatic islet cell types (α and β cells) were created, with this last pattern extended into three dimensions through the transfer of patterned cells into thin, stackable PEG hydrogel films. Cell viability was confirmed in both patterns, and cell function was established in the islet cell design through the on-chip detection of insulin secretion. This platform is scalable and can naturally accommodate the multiplexed patterning of an expanded number of distinct cell types. This technology could have applications for tissue-engineered implants, cell-based assays, and fundamental studies of tissue microenvironments.

Received: March 31, 2011
Published online: June 29, 2011

**Keywords:** cell assembly · flow-patterning · microarrays · microfluidics · tissue engineering

[1] C. Chen, M. Mrksich, S. Huang, G. Whitesides, D. Ingber, *Science* **1997**, *276*, 1425.
[2] T. Boland, V. Mironov, A. Gutowska, E. Roth, R. Markwald, *Anat. Rec. Part A* **2003**, *272*, 497–502.
[3] T. Xu, J. Jin, C. Gregory, J. Hickman, T. Boland, *Biomaterials* **2005**, *26*, 93–99.
[4] A. Folch, B. Jo, O. Hurtado, D. Beebe, M. Toner, *J. Biomed. Mater. Res. Part A* **2000**, *52*, 346–353.
[5] D. Albrecht, G. Underhill, T. Wassermann, R. Sah, S. Bhatia, *Nat. Methods* **2006**, *3*, 369–375.
[6] A. Rosenthal, J. Voldman, *Biophys. J.* **2005**, *88*, 2193–2205.
[7] E. Dufresne, D. Grier, *Rev. Sci. Instrum.* **1998**, *69*, 1974.
[8] M. Ozkan, T. Pisanic, J. Scheel, C. Barlow, S. Esener, S. Bhatia, *Langmuir* **2003**, *19*, 1532–1538.
[9] R. Fan, O. Vermesh, A. Srivastava, B. Yen, L. Qin, H. Ahmad, G. Kwong, C. Liu, J. Gould, L. Hood, J. R. Heath, *Nat. Biotechnol.* **2008**, *26*, 1373–1378.
[10] G. G. Borisenko, M. A. Zaitseva, A. N. Chuvilin, G. E. Pozmogova, *Nucleic Acids Res.* **2009**, *37*, e28.
[11] S. Hsiao, B. Shum, H. Onoe, E. Douglas, Z. Gartner, R. Mathies, C. Bertozzi, M. Francis, *Langmuir* **2009**, *25*, 6985–6991.
[12] G. Kwong, C. Radu, K. Hwang, C. Shu, C. Ma, R. Koya, B. Comin-Anduix, S. Hadrup, R. Bailey, O. Witte, J. R. Heath, *J. Am. Chem. Soc.* **2009**, *131*, 9695–9703.
[13] V. Ramachandiran, V. Grigoriev, L. Lan, E. Ravkov, S. A. Mertens, J. D. Altman, *J. Immunol. Methods* **2007**, *319*, 13–20.
[14] V. A. Liu, S. N. Bhatia, *Biomed. Microdevices* **2002**, *4*, 257–266.

  